RESEARCH PAPER

Postsynaptic mechanisms underlying the excitatory action of histamine on medial vestibular nucleus neurons in rats

Xiao-Yang Zhang[†], Lei Yu[†], Qian-Xing Zhuang[†], Shi-Yu Peng, Jing-Ning Zhu and Jian-Jun Wang

Department of Biological Science and Technology and State Key Laboratory of Pharmaceutical Biotechnology, School of Life Sciences, Nanjing University, Nanjing, China

BACKGROUND AND PURPOSE

Anti-histaminergic drugs have been widely used in the clinical treatment of vestibular disorders and most studies concentrate on their presynaptic actions. The present study investigated the postsynaptic effect of histamine on medial vestibular nucleus (MVN) neurons and the underlying mechanisms.

EXPERIMENTAL APPROACH

Histamine-induced postsynaptic actions on MVN neurons and the corresponding receptor and ionic mechanisms were detected by whole-cell patch-clamp recordings on rat brain slices. The distribution of postsynaptic histamine H_1, H_2 and H_4 receptors was mapped by double and single immunostaining. Furthermore, the expression of mRNAs for H_1, H_2 and H_4 receptors and for subtypes of Na^+–Ca^{2+} exchangers (NCXs) and hyperpolarization-activated cyclic nucleotide-gated (HCN) channels was assessed by quantitative real-time RT-PCR.

KEY RESULTS

A marked postsynaptic excitatory effect, co-mediated by histamine H_1 and H_2 receptors, was involved in the histamine-induced depolarization of MVN neurons. Postsynaptic H_1 and H_2 rather than H_4 receptors were co-localized in the same MVN neurons. NCXs contributed to the inward current mediated by H_1 receptors, whereas HCN channels were responsible for excitation induced by activation of H_2 receptors. Moreover, NCX1 and NCX3 rather than NCX2, and HCN1 rather than HCN2-4 mRNAs, were abundantly expressed in MVN.

CONCLUSION AND IMPLICATIONS

NCXs coupled to H_1 receptors and HCN channels linked to H_2 receptors co-mediate the strong postsynaptic excitatory action of histamine on MVN neurons. These results highlight an active role of postsynaptic mechanisms in the modulation by central histaminergic systems of vestibular functions and suggest potential targets for clinical treatment of vestibular disorders.

LINKED ARTICLES

This article is part of a themed issue on Histamine Pharmacology Update. To view the other articles in this issue visit http://dx.doi.org/10.1111/bph.2013.170.issue-1

Abbreviations

HCN channels, hyperpolarization-activated cyclic nucleotide-gated channels; ISIs, interspike intervals; *I–V* curves, current–voltage plots; MVN, medial vestibular nucleus; NCXs, Na^+–Ca^{2+} exchangers; PSTHs, peri-stimulus time histograms

Introduction

Anti-histaminergic drugs have been widely used in the clinical treatment of vestibular disorders and symptoms, including vertigo, motion sickness, nausea and nystagmus (Lacour and Sterkers, 2001; Bergquist and Dutia, 2006; Haas *et al.*, 2008; Tiligada *et al.*, 2011). The medial vestibular nucleus (MVN) is the most relevant subnucleus in the vestibular nuclear complex in the brainstem. The MVN occupies a key position in the stabilization, coordination and compensation of head and eye movements (Straka *et al.*, 2005; Highstein and Holstein, 2006) and is considered to be the most critical central target for anti-histaminergic drugs. However, the physiological and therapeutic mechanisms by which histaminergic agents modulate vestibular functions, particularly the detailed mechanisms underlying the action of histamine on the MVN, remain largely unknown.

Recent years have witnessed significant progress in the role of presynaptic histamine H_3 receptors (receptor and channel nomenclature follows Alexander *et al.*, 2011) in central vestibular nuclei-related reflexes, especially in vestibular compensation, i.e., the recovery process to regain balance control and minimize dizziness symptoms following peripheral vestibular lesion (Bergquist and Dutia, 2006; Bergquist *et al.*, 2006; Tighilet *et al.*, 2006; 2007). However, intriguingly, apart from betahistine, generally considered to be a H_3 receptor antagonist, several antagonists for postsynaptic histamine H_1 receptors, such as meclizine and flunarizine (Hain and Uddin, 2003; Lacour, 2006), are also quite effective in preventing and treating vertigo and motion sickness. Betahistine itself is known to exert a weak agonist effect on H_1 receptors (Wang and Dutia, 1995; Lacour and Sterkers, 2001).

On the other hand, several studies indicate a role of postsynaptic H_1 and H_2 receptors in histaminergic neurotransmission in central vestibular nuclei. In rats and guinea pigs, both histamine H_1 and H_2 receptors are expressed in the vestibular nuclei (Palacios *et al.*, 1981; Bouthenet *et al.*, 1988; Ruat *et al.*, 1991; Vizuete *et al.*, 1997). Moreover, H_2 and/or H_1 receptors mediated the excitatory effect of histamine on the MVN neurons *in vivo* and *in vitro* (Serafin *et al.*, 1993; Yabe *et al.*, 1993; Wang and Dutia, 1995).

Thus, the postsynaptic action of histamine on the vestibular nuclei, particularly on the MVN, and the underlying mechanisms should not be overlooked in attempts to understand the physiological and pathophysiological significance of the histaminergic modulation of vestibular functions. In the present study, by using whole-cell patch-clamp recordings, quantitative real-time RT-PCR and immunostaining, the postsynaptic mechanisms of histamine on MVN neurons, were investigated. Here, we show that Na^+–Ca^{2+} exchangers (NCXs) coupled to H_1 receptors and hyperpolarization-activated cyclic nucleotide-gated (HCN) channels linked to H_2 receptors co-mediate the postsynaptic depolarization of MVN neurons by histamine.

Methods

Whole-cell patch-clamp recordings

All animal care and experimental procedures complied with the US National Institutes of Health Guide for the Care and Use of Laboratory Animals (NIH Publication 80-23, revised 1996) and are reported in accordance with the ARRIVE guidelines (McGrath *et al.*, 2010). For these experiments, we used 53 Sprague-Dawley rats (Experimental Animal Center of Nanjing Medical University, Nanjing, China) of either sex aged 14–21 days because the histaminergic fibres reach an adult-like appearance about 2 weeks post-natally (Haas *et al.*, 2008). The rats were decapitated under sodium pentobarbital (40 mg·kg^{-1}) anaesthesia. After carefully removing the skull, the brainstem extending from obex to the superior colliculi was rapidly removed into ice-cold artificial CSF (ACSF, composition in mM: 124 NaCl, 2.5 KCl, 1.25 NaH$_2$PO$_4$, 1.3 MgSO$_4$, 26 NaHCO$_3$, 2 CaCl$_2$ and 10 D-glucose) equilibrated with 95% O$_2$ and 5% CO$_2$. According to the rat brain atlas (Paxinos and Watson, 2007), coronal slices (300 μM in thickness) of brainstem containing the MVN were cut with a vibroslicer (VT 1200 S, Leica Microsystems, Wetzlar, Germany) and the nucleus was identified. The slices were incubated in 95% O$_2$ and 5% CO$_2$ oxygenated ACSF at 35 ± 0.5°C for at least 1 h and then maintained at room temperature. During recording sessions, the slices were transferred to a submerged chamber and continuously perfused with 95% O$_2$ and 5% CO$_2$ oxygenated ACSF at a rate of 2 mL·min^{-1} maintained at room temperature.

Whole-cell patch-clamp recordings were performed as previously described (Zhang *et al.*, 2008; 2011) on MVN neurons with borosilicate glass pipettes (3–5 MΩ) filled with an internal solution (composition in mM: 140 K methylsulfate, 7 KCl, 2 MgCl$_2$, 10 HEPES, 0.1 EGTA, 4 Na$_2$ ATP, 0.4 GTP-Tris, adjusted to pH 7.25 with 1 M KOH). During recording sessions, MVN neurons were visualized with an Olympus BX51WI microscope (Olympus, Tokyo, Japan). Patch-clamp recordings were acquired with an Axopatch-200B amplifier (Axon Instruments, Foster City, CA, USA) and the signals were fed into a computer through a Digidata-1322A interface (Axon Instruments) for data capture and analysis (pClamp 8.2, Axon Instruments). Recordings of whole-cell currents were low-pass filtered at 2 kHz and digitized at 10 kHz and recordings of membrane potentials were low-pass filtered at 5 kHz and digitized at 20 kHz. The interspike interval (ISI, sampling interval = 1 ms) distributions and the peri-stimulus time histograms (PSTHs) of the recorded neuronal discharges were generated by computer to assess the effects of drugs on the cells. Neurons were held at a membrane potential of −60 mV and characterized by injection of rectangular voltage pulse (5 mV, 50 ms) to monitor the whole-cell membrane capacitance, series resistance and membrane resistance. Neurons were excluded from the study if the series resistance was not stable or exceeded 20 MΩ.

We bathed the slices with histamine (1–100 μM, Sigma, St. Louis, MO, USA) to stimulate the recorded neurons. TTX (0.3 μM, Alomone Labs, Jerusalem, Israel) was used to confirm and isolate the postsynaptic effect of histamine. Selective antagonists for histamine H_1, H_2 and H_4 receptors, mepyramine (1 μM, Tocris, Bristol, UK), ranitidine (1 μM, Tocris), and JNJ7777120 (10 μM, a kind gift from Dr. Rob Leurs, VU University Amsterdam, Amsterdam, the Netherlands), as well as selective agonists for the H_1 receptor -, 2-(2-pyridyl)ethylamine (2-PyEA; 10–300 μM, Sigma), for the H_2 receptor – dimaprit (30–1000 μM, Tocris) and for the H_4 receptor – VUF8430 (300–1000 μM, a kind gift from Dr. Rob Leurs,

VU University Amsterdam) were applied to assess the underlying postsynaptic receptor mechanisms. 2-PyEA and dimaprit were used to separate the inward current mediated by postsynaptic H_1 and H_2 receptors respectively. To characterise the 2-PyEA- and dimaprit-induced whole cell current and the underlying ionic mechanisms, in voltage-clamp recording, current–voltage plots (I–V curves) were obtained before and during drug application using a slow ramp command ($dV/dt = -10$ mV·s^{-1}, ranged from -60 to -120 mV) to allow for attainment of steady-state conditions (Wu et al., 2004; Zhang et al., 2011). KB-R7943 (50 μM, Tocris), BaCl$_2$ (1 mM) and ZD7288 (50 μM, Tocris) were applied to block the NCXs, K$^+$ channels and HCN channels respectively. Furthermore, Na$^+$ replacement was conducted by using Tris$^+$ to inactivate NCXs. The composition of the Tris$^+$ ACSF was as follows (in mM): 124 Tris–Cl, 2.5 KCl, 1.25 NaH$_2$PO$_4$, 1.3 MgSO$_4$, 26 NaHCO$_3$, 2 CaCl$_2$ and 10 D-glucose. Depolarizing voltage sag generated by activation of HCN channels in response to hyperpolarizing current steps (70–150 pA, 1 s) in the absence and presence of dimaprit was measured in current-clamp recordings. The amplitude of voltage sag was calculated by subtracting the peak voltage amplitude from the steady-state voltage.

Before bath application of histaminergic compounds at known concentrations, the whole-cell current of the recorded neuron was observed for at least 20 min to assure stability. Histamine or a histamine receptor agonist was added to the perfusing ACSF to stimulate the recorded neuron for a test period of 1 min. After each stimulation, cells were given at least 20 min for recovery and to avoid desensitization. The antagonists or blockers were given for at least 15 min before we observed their effects.

Immunofluorescence

The experimental procedures for immunostaining followed our previous reports (Zhang et al., 2011; Peng et al., 2013; Zhuang et al., 2013). Rats (weighing 230–250 g) were deeply anaesthetized with sodium pentobarbital and perfused transcardially with 100 mL of normal saline, followed by 450–500 mL of 4% paraformaldehyde in 0.1 M phosphate buffer. Subsequently, the brain was removed, trimmed and postfixed in the same fixative for 12 h at 4°C, and then cryoprotected with 30% sucrose for 48 h. Frozen coronal sections (25 μm thick) containing the MVN were obtained by using a freezing microtome (CM 3050S, Leica Microsystems) and mounted on gelatin-coated slides. The slices were rinsed with PBS containing 0.1% Triton X-100 (PBST) and then incubated in 10% normal bovine serum in PBST for 30 min. Sections were incubated overnight at 4°C with primary antibodies to histamine H_1 (a rabbit anti-H_1 receptor polyclonal antibody, 1:50; Santa Cruz Biotechnology, Santa Cruz, CA, USA) and H_2 receptors (a goat anti-H_2 receptor polyclonal antibody, 1:200; Everest Biotech, Oxfordshire, UK), or a primary antibody to H_4 receptors (a rabbit anti-H_4 receptor polyclonal antibody, 1:50; Santa Cruz Biotechnology) respectively. After a complete wash in PBS, the former was incubated in the Alexa 594-conjugated donkey anti-rabbit (1:2000; Invitrogen, Carlsbad, CA, USA) and Alexa 488-conjugated donkey anti-goat (1:2000; Invitrogen), while the latter was incubated in the Alexa 488-conjugated goat anti-rabbit (1:2000; Invitrogen), respectively, for 2 h at room temperature in the dark. The slides were washed and mounted in UltraCruz mounting medium (Santa Cruz Biotechnology). All micrographs were taken with an inverted laser scanning confocal microscope (FV1000; Olympus). Incubations replacing the primary antiserum with control immunoglobulins and/or omitting the primary antiserum were used as negative controls.

Quantitative real-time RT-PCR

For this experiment, three independent groups of RNA pools each from five animals were used as biological replicates. MVN tissue punches were collected from coronal brain slices of Sprague-Dawley rats (weighing 230–250 g) according to the rat brain atlas of Paxinos and Watson (2007) and pooled (5 animals in each pool). RNA extraction was carried using TriZol reagent (Invitrogen) according to the manufacturer's instructions. A 1 μg aliquot of total RNA was used for the first-strand cDNA synthesis according to the protocol of M-MLV reverse transcriptase (Promega, Madison, WI, USA). Real-time PCR was then performed using iQ SYBR Green SuperMix (Bio-Rad, Hercules, CA, USA) in a 20 μL of reaction mixture containing 10 μL of 2× master mix, 2 μL of cDNA, 2 μL of each primer (5 μM) and 4 μL of distilled water. The reaction was carried out in a Bio-Rad CFX-96 real-time PCR system using the following parameters: 95°C for 3 min to activate the hot-start iTaq DNA polymerase, followed by 40 cycles at 95°C for 15 s, 60°C for 25 s and 72°C for 1 s. The PCR programme was completed by a melting temperature analysis. For quantification, the quantity of the target gene was expressed relative to the amount of the reference gene (gapdh) to obtain a normalized target expression value. For negative controls, cDNA was replaced with water. Primer sequences summarized in Table 1 except for those for HCN2 are all from previous reports (Lu et al., 2002; Lazarov et al., 2006; Bolívar et al., 2008; Atherton et al., 2010).

Data analysis

All data were analysed with Origin 7.5 (MicroCal Software, Northampton, MA, USA) and expressed as means ± SEM. Student's t-test was employed for statistical analysis of the data and P-values of <0.05 were considered to be significant.

Results

A marked postsynaptic excitatory component in the histamine-induced excitation on MVN neurons

A total of 76 MVN neurons with input resistance higher than 300 MΩ, capacitance of 153.5 ± 25.7 pF and spontaneous discharge rate of 12.4 ± 4.1 spikes·s^{-1}, were recorded in the present study. According to the shapes of the afterhyperpolarization action potential reported previously (Serafin et al., 1991; Johnston et al., 1994; Beraneck et al., 2003), the 76 recorded MVN neurons were classified as either type A (n = 26) or type B (n = 50) neurons. Histamine excited both types of the recorded neurons (76/76, 100%).

In the current clamp experiments, brief bath application (1 min) of 30 μM histamine elicited a significant excitatory response on the MVM neurons (Figure 1A) with an increase of peak firing rate by 74 ± 11% (n = 7). The ISIs and PSTHs showed that histamine largely shortened the intervals of the

Table 1

Sequences of oligonucleotide primers used for PCR amplification

Primers	Sequences (5′–3′)	Sources
H_1p1	CCTCTACCTTCGAAGACAAG	NM017018
H_1p2	GTCTTGGTTCGGTACCTCAG	
H_2p1	ATGGCATTGAAAGTCACC	NM012965
H_2p2	GACCAAAGAGATGGCAAC	
H_4p1	TAACGATAGGCAATGCTGTG	NM131909
H_4p2	TCTTCCAAGAATCCGAAGCC	
NCX1p1	ACCACCAAGACTACAGTGCG	X68813
NCX1p2	TTGGAAGCTGGTCTGTCTCC	
NCX2p1	GGGCACTGAGGTCCCAGGCGAGCT	U08141
NCX2p2	CAGCAGCCTCACGAAGAAGTGCTC	
NCX3p1	CAGACTGCAAGGAGGGTGTC	U53420
NCX3p2	AATCACCAGCAATGAACCCG	
HCN1p1	ATGCCTCTCTTTGCTAACGC	NM 053375
HCN1p2	TATTCCTCCAAGACCTCGTTGAA	
HCN2p1	CTACAGCGACTTCAGGTTCTACTGGG	NM 053684
HCN2p2	GACCACGTTGAAGACGATCCAGG	
HCN3p1	GTCGGAGAACAGCCAGTGTAA	NM 053685
HCN3p2	TGAGCGTCTAGCAGATCGAG	
HCN4p1	ATCAACGGCATGGTGAATAACTC	NM 021658
HCN4p2	TGCCCTGGTAGCGGTGTTC	
GAPDHp1	GGTGCTGAGTATGTCGTGGAGTCTAC	NM 017008
GAPDHp2	CATGTAGGCCATGAGGTCCACCACC	

spikes and increased the firing rate of the MVN neurons (Figure 1B,C). Moreover, when perfusing the slices with ACSF containing 0.3 μM TTX, 30 μM histamine still evoked a strong depolarization of 5.1 ± 0.7 mV on the MVN neurons (n = 5), suggesting a marked postsynaptic excitatory effect induced by histamine (Figure 1D). On the other hand, in voltage-clamp experiments in TTX, histamine elicited stable inward whole-cell currents on the MVN neurons (Figure 1E), confirming a postsynaptic excitatory action of histamine on the cells. In addition, the histamine-induced postsynaptic excitation was concentration-dependent (Figure 1E). Fitting the concentration–response curves from type A (n = 5) and type B (n = 5) MVN neurons provided EC_{50} values for histamine of 7.1 and 5.7 μM respectively (Figure 1F).

H_1 and H_2 receptors co-mediate the histamine-induced postsynaptic excitation on MVN neurons

Histamine exerts its action via four distinct receptor subtypes. The histamine H_1, H_2 and H_4 receptors are postsynaptic, whereas H_3 receptors are mostly presynaptic with some post-synaptic locations (Brown *et al.*, 2001; Pillot *et al.*, 2002; Haas and Panula, 2003; Haas *et al.*, 2008). However, in the MVN, H_3 receptors are considered to exert an important presynaptic role (Lacour and Sterkers, 2001; Lozada *et al.*, 2004; Bergquist and Dutia, 2006; Bergquist *et al.*, 2006). Therefore, in the

present study, we used selective histamine H_1, H_2 and H_4 receptor antagonists to examine which postsynaptic histamine receptor(s) mediated the histamine-induced excitation on MVN neurons (Figures 2 and 3). As shown in Figure 2A–C, in the presence of 0.3 μM TTX, the 30 μM histamine-induced inward currents were partly blocked by separate application of mepyramine or ranitidine, highly selective receptor antagonists for H_1 and H_2 receptors, respectively, and totally antagonized by combined application of mepyramine and ranitidine, indicating a dual receptor mechanism involved in the histamine-induced postsynaptic excitation. Furthermore, quantitative real-time RT-PCR data revealed that both histamine H_1 and H_2 receptor mRNAs were abundantly expressed in the MVN (Figure 2D), and double immunostaining results showed that histamine H_1 and H_2 receptors were not only present in the rat MVN but also co-localized in the same MVN neurons (Figure 2E1–2G3).

We also assessed the role of histamine H_4 receptors in the postsynaptic excitatory effect of histamine on MVN neurons. This receptor is the most recently cloned histamine receptor and is located postsynaptically in brain and peripheral tissues (Connelly *et al.*, 2009; Strakhova *et al.*, 2009; Lethbridge and Chazot, 2010). JNJ7777120 (10 μM), a highly selective H_4 receptor antagonist (Jablonowski *et al.*, 2003), had no effect on histamine-induced inward current and VUF8430 (300 μM or 1 mM), a highly selective H_4 receptor agonist (Lim *et al.*, 2006), did not mimic the histamine-induced postsynaptic excitation on MVN neurons (n = 5; Figure 3A,B). Moreover, both histamine H_4 receptor mRNAs and proteins were not detected in the rat MVN (Figures 2D and 3C1–3D3). All these results strongly suggest that histamine H_1 and H_2 rather than H_4 receptors co-mediate the postsynaptic excitatory component induced by histamine on MVN neurons. Furthermore, no difference was found in the postsynaptic receptor mechanisms of histamine between type A (n = 6) and type B (n = 13) MVN neurons.

NCXs mediate the excitation induced by activation of H_1 receptors on MVN neurons

Given the finding of the dual receptor mechanism underlying the histamine-induced inward current on MVN neurons, we employed 2-PyEA and dimaprit, highly selective agonists for histamine H_1 and H_2 receptors, respectively, to determine the ionic fluxes separately coupled to H_1 and H_2 receptors. As shown in Figure 4A, 2-PyEA (10–300 μM) mimicked the histamine-induced excitatory effect in a concentration-dependent manner. Fitting the concentration–response curve from 7 MVN neurons yielded an EC_{50} value for 2-PyEA of 46.7 μM. The 2-PyEA-induced inward current was totally blocked by mepyramine (Figure 4B,C), indicating 2-PyEA evoked an isolated current associated with activation of post-synaptic H_1 receptors.

Next, we determined the $I–V$ curves in response to 2-PyEA to investigate the ionic mechanism underlying its effects on MVN neurons. We employed slow ramp command tests (dV/dt = –10 mV·s^{-1}, ranged from –60 to –120 mV) to evaluate the $I–V$ curves for a large voltage range in the absence and presence of 2-PyEA. As shown in Figure 4D, the 2-PyEA-induced inward current had a larger amplitude at –120 mV as compared with –60 mV and the two curves showed a trend of intersection at a potential more depolarized than –60 mV
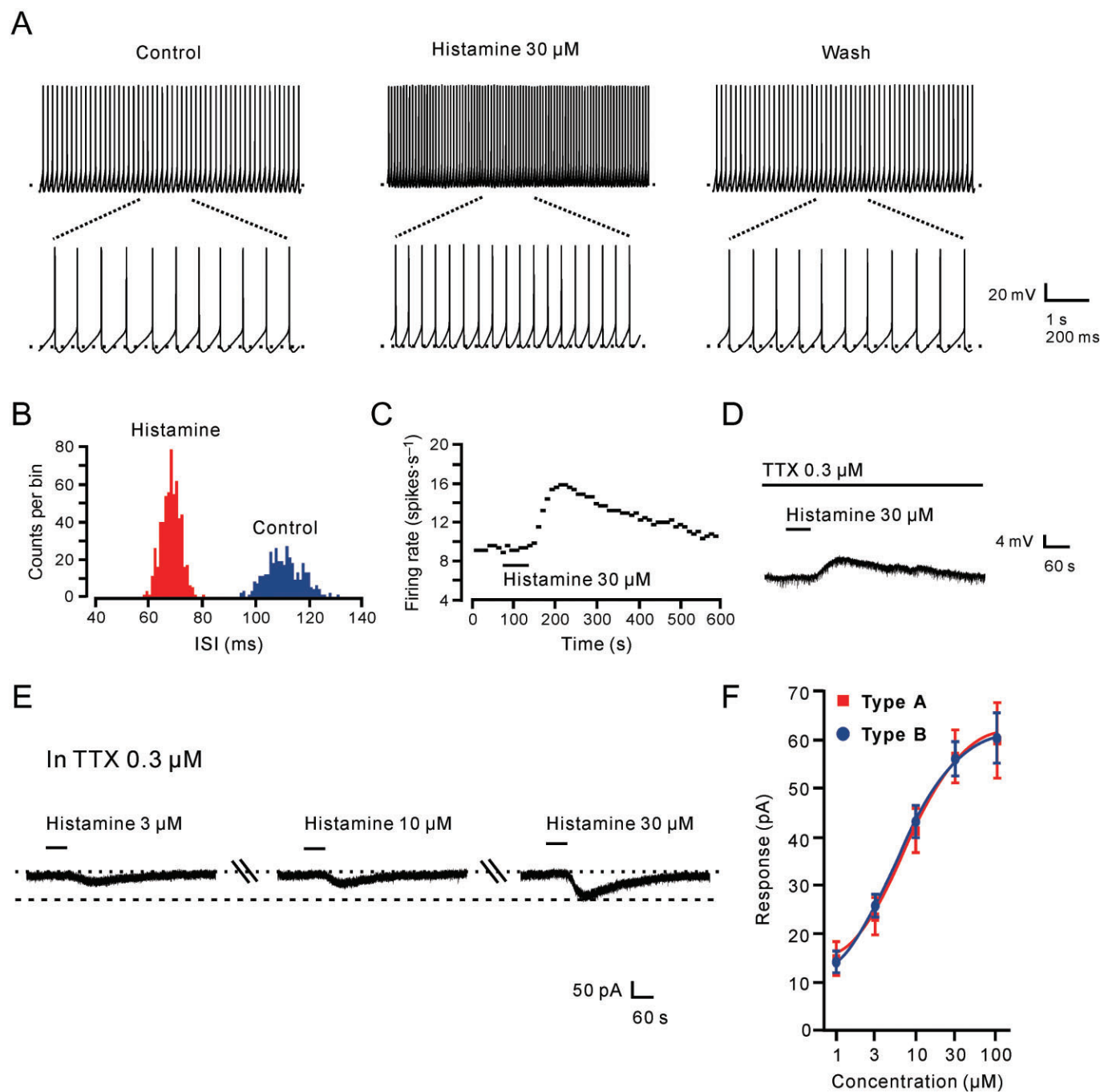
A

Control   Histamine 30 µM   Wash

20 mV
1 s
200 ms

B Histamine / Control   ISI (ms), Counts per bin

C Firing rate (spikes·s⁻¹), Time (s), Histamine 30 µM

D TTX 0.3 µM, Histamine 30 µM, 4 mV, 60 s

E In TTX 0.3 µM   Histamine 3 µM   Histamine 10 µM   Histamine 30 µM   50 pA, 60 s

F Type A, Type B, Response (pA), Concentration (µM)

Figure 1

A marked postsynaptic excitatory component was involved in the histamine-induced excitation of MVN neurons. (A) Histamine excited a MVN neuron. Analysis of the ISI (B) and PSTH (C) showed that histamine shortened the ISI and increased the firing rate of the MVN neuron presented in (A). (D) Histamine still induced strong depolarization of the same MVN neuron in the presence of TTX. (E) Histamine dose-dependently elicited an inward current in a MVN neuron. (F) Concentration–response curves for histamine on recorded type A ($n = 5$) and type B ($n = 5$) MVN neurons shows the mean EC_{50} value for histamine of 7.1 and 5.7 µM, respectively. In this and the following figures, the short horizontal bars above the experimental records indicate the 1 min period of application of histamine or histamine receptor agonist, and the long horizontal bars indicate the exposure of the slice to TTX, histamine receptor antagonist or blockers of ion exchangers or channels.

($n = 5$). Subtracting the control from the current recorded during 2-PyEA application yielded a difference current representing the 2-PyEA-induced current (the right panel of Figure 4D).

Among the various ionic mechanisms coupled to histamine H_1 receptors in different brain regions, NCXs have a more positive reversal potential (Wu *et al.*, 2004; Zhang *et al.*, 2011). Therefore, we applied KB-R7943, a blocker of NCXs, to

the MVN neurons. In the presence of 50 μM KB-R7943 in the slow ramp command tests (Figure 4E), the *I–V* curve recorded during 2-PyEA application coincided with that recorded in the absence of 2-PyEA and the 2-PyEA-induced current disappeared. Furthermore, in gap-free mode, which is used to acquire continuous data without giving any stimulus pulses, the 2-PyEA-induced inward current was abolished by KB-R7943 (Figure 5A,B). Moreover, we tested the effect of replacing the external Na^+ with equimolar concentrations of $Tris^+$, a relatively large organic cation that should not support Na^+-dependent currents for investigating Na^+-dependent ionic mechanisms, including electrogenic NCXs (with 3 Na^+ ions entering in exchange for 1 Ca^{2+} ion). As shown in Figure 5C and 5D, replacement of external Na^+ with $Tris^+$ totally blocked the 2-PyEA-induced inward current at –60 mV confirming the contribution of NCXs coupled to histamine H_1 receptors. As K^+ currents are also an important component involved in excitation induced by activation of H_1 receptors (Brown *et al.*, 2001; Haas and Panula, 2003), we perfused the slices with ACSF containing Ba^{2+} (1 mM $BaCl_2$), a broad spectrum blocker of K^+ channels, and found that Ba^{2+} had no influence on the inward currents induced by 300 μM 2-PyEA (Figure 5E,F). The results indicate that NCXs mediate the excitatory effect of activation of histamine H_1 receptors on MVN neurons. Furthermore, there was no difference in the ionic mechanisms coupled to histamine H_1 receptors between type- A (*n* = 7) and type B (*n* = 13) MVN neurons.

Three NCX subtypes (NCX1, NCX2 and NCX3) have been identified and all are expressed in the brain (Annunziato *et al.*, 2004). Therefore, we further assessed the expression of NCX1-3 mRNAs in rat MVN by quantitative real-time RT-PCR. The results showed that NCX1 and NCX3 rather than NCX2 mRNAs were abundantly expressed in the MVN (Figure 5G), indicating that NCX1 and NCX3 may contribute to the histamine H_1-receptor-induced excitatory effect on MVN neurons.

HCN channels mediate the excitation induced by activation of H_2 receptors on MVN neurons

We employed dimaprit to isolate histamine H_2-receptor-induced inward current on MVN neurons to further determine the ionic mechanisms coupled to H_2 receptors. As shown in Figure 6A, dimaprit (30–1000 μM) also concentration-dependently mimicked the histamine-induced excitatory effect, as observed with 2-PyEA. Fitting the concentration–response curve from 5 MVN neurons yielded an EC_{50} value for dimaprit of 157.7 μM. The inward current induced by dimaprit-activated H_2 receptors was also totally blocked by ranitidine (Figure 6B,C).

We used slow ramp command tests to obtain the *I–V* curves in the absence and presence of dimaprit (the left panel of Figure 6D). The difference current representing the dimaprit-induced current (the right panel of Figure 6D) from the 5 MVN neurons exhibited a significant feature of hyperpolarization activation, which is consistent with the characteristics of HCN channels (Pape, 1996). After blockade of HCN channels with ZD7288, the dimaprit-induced net current was abolished (Figure 6E). ZD7288 (50 μM) also totally blocked the inward current induced by dimaprit

(300 μM) in a gap-free mode (Figure 7A,B). Moreover, as one of the hallmarks of HCN channel activation is the depolarizing voltage sag generated during the course of negative voltage deviations in current clamp recording (Pape, 1996), we further tested the effect of dimaprit on voltage sag in recording cells in response to hyperpolarizing current steps (70–150 pA, 1 s). The result showed that dimaprit increased the depolarizing sag (Figure 7C,D), confirming that HCN channels mediated the effect of activation of H_2 receptors. In addition, no difference was found in ion channels coupled to histamine H_2 receptors between type A (*n* = 6) and type B (*n* = 9) MVN neurons.

Four subtypes of HCN channels (HCN1, HCN2, HCN3 and HCN4) have been cloned and they are all expressed in the brain (Notomi and Shigemoto, 2004). Therefore, we further assessed the expression of HCN1-4 mRNAs in rat MVN by quantitative real-time RT-PCR. The results showed that HCN1 rather than HCN2-4 mRNAs were abundantly expressed in the rat MVN (Figure 7E), indicating that the histamine H_2-receptor-induced excitatory effect on MVN neurons is mainly mediated via HCN1 channels.

To confirm our data relating to the postsynaptic ionic mechanisms underlying histamine-induced excitation on MVN neurons, ZD7288 was applied in combination with KB-R7943. As shown in Figure 7F and 7G, in the presence of 0.3 μM TTX, combined application of ZD7288 (50 μM) and KB-R7943 (50 μM) totally blocked the postsynaptic inward current induced by 30 μM histamine. The results, together with the data shown in Figures 4–6, strongly suggested that NCXs coupled to H_1 receptors and HCN channels linked to H_2 receptors co-mediated the postsynaptic depolarization of histamine on both type A and type B neurons of the MVN.

Discussion

Histamine has traditionally been considered to hold a key position in central and peripheral vestibular functions. Among the vestibular nuclei in the brainstem, itself a sensorimotor complex integrating vestibular, visual and motor signals to make compensatory eye and head movements as well as postural adjustments, the MVN, receiving inputs primarily from the semicircular canals, not only innervates cervical motor neurons to stabilize the position of the head in space, but also sends axons into the medial longitudinal fasciculus to participate in vestibulo-ocular reflexes (Straka *et al.*, 2005; Highstein and Holstein, 2006). Studies from our laboratory and others have already documented that histamine exerts an excitatory role in all four major sub-nuclei in the vestibular nuclear complex (Zhang *et al.*, 2008; Zhuang *et al.*, 2013) including the MVN (Wang and Dutia, 1995), and extensively modulates the vestibular-related reflexes (Yabe *et al.*, 1993; Lacour and Sterkers, 2001; Bergquist and Dutia, 2006). However, receptor mechanisms underlying this homogeneous excitatory effect of histamine on four vestibular sub-nuclei are different and the ionic basis is still largely unknown. In the present study, we have described a strong postsynaptic depolarization/excitation of histamine on the MVN neurons. This effect was mediated by postsynaptic histamine H_1 and H_2 rather than H_4 receptors. NCXs coupled to
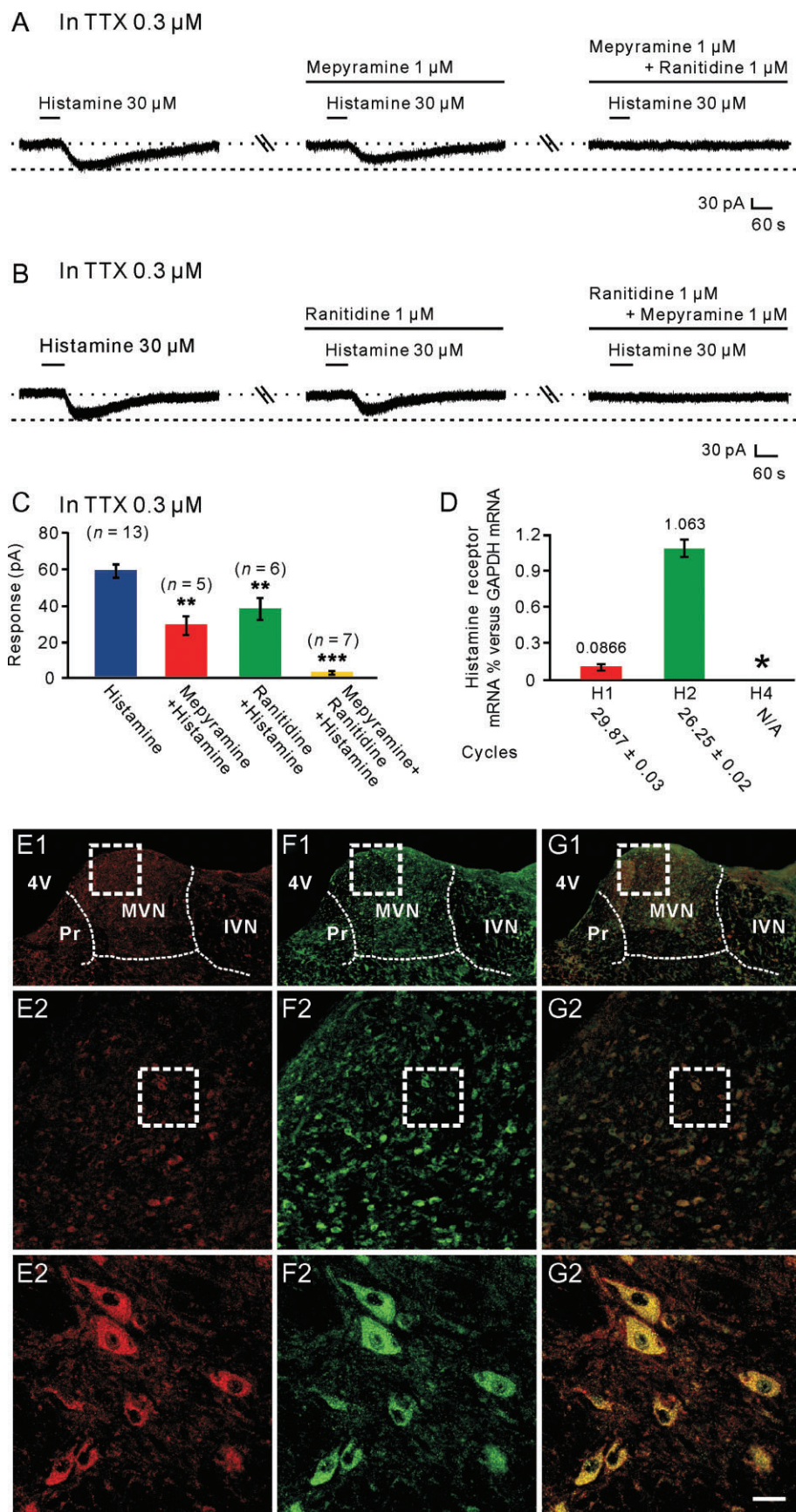
A In TTX 0.3 μM

Histamine 30 μM

Mepyramine 1 μM
Histamine 30 μM

Mepyramine 1 μM
+ Ranitidine 1 μM
Histamine 30 μM

30 pA
60 s

B In TTX 0.3 μM

Histamine 30 μM

Ranitidine 1 μM
Histamine 30 μM

Ranitidine 1 μM
+ Mepyramine 1 μM
Histamine 30 μM

30 pA
60 s

C In TTX 0.3 μM

D

Figure 2

H_1 and H_2 receptors co-mediated the histamine-induced postsynaptic excitation on MVN neurons. (A) In the presence of TTX, the histamine-induced inward currents were partly blocked by mepyramine, a highly selective H_1 receptor antagonist, and abolished by combined application of mepyramine and ranitidine, a highly selective H_2 receptor antagonist. (B) In the presence of TTX, the histamine-induced inward currents were partly blocked by ranitidine, and abolished by the combination of mepyramine and ranitidine. (C) Group data of the tested MVN neurons. Data shown are means ± SEM; **$P < 0.01$, ***$P < 0.001$, significantly different from control. (D) Bar graphs showing the relative expression of H_1, H_2 and H_4 receptor mRNAs in the MVN. In this and the following figures, asterisks indicate samples showing no specific signal, and cycles necessary to get a signal are listed below each gene. (E1–G3) Double immunostaining results showed that histamine H_1 (E1–E3) and H_2 (F1–F3) receptors were not only present in the rat MVN but also co-localized in the same MVN neurons (G1–G3). Scale bars: (C1), (D1) and (E1), 550 μm; (C2), (D2) and (E2), 100 μm; (C3), (D3) and (E3), 20 μm. 4V, 4th ventricle; IVN, inferior vestibular nucleus; MVN, medial vestibular nucleus; Pr, prepositus nucleus.
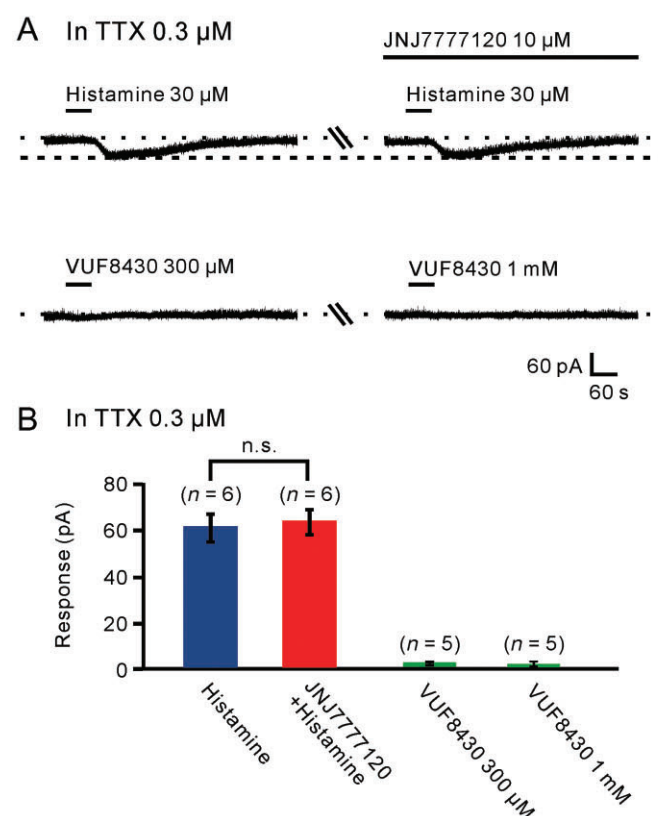

Figure 3

H_4 receptors are not involved in the postsynaptic excitatory effect of histamine on MVN neurons. (A) JNJ7777120, a highly selective H_4 receptor antagonist, had no effect on histamine-induced inward current, and VUF8430, a highly selective H_4 receptor agonist, did not mimic the histamine-induced postsynaptic excitation on MVN neurons. (B) Group data of the tested MVN neurons. Data shown are means ± SEM. (C1–C3) Histamine H_4 receptor-immunolabelled neurons were not detected in the rat MVN. (D1–D3) Negative staining controls. n.s. indicates non-significant. Scale bars: (C1) and (D1), 550 μm; (C2) and (D2), 100 μm; (C3) and (D3), 20 μm. 4V, 4th ventricle; IVN, inferior vestibular nucleus; MVN, medial vestibular nucleus; Pr, prepositus nucleus.

H_1 receptors and the HCN channels coupled to H_2 receptors contributed to the postsynaptic excitatory effect of histamine on MVN neurons.

In the brain, the actions of histamine are mediated by G-proteins and various second messenger pathways and ionic mechanisms (Brown *et al.*, 2001; Haas and Panula, 2003; Haas *et al.*, 2008). In the MVN, low threshold calcium channels, BK type calcium-activated potassium channels, K_v3 family of potassium channels and other types of channels have been reported previously to regulate the excitability of neurons in the nucleus (Serafin *et al.*, 1990; Gittis and du Lac, 2007; 2008; Gittis *et al.*, 2010). However, histamine modulates MVN neurons by activation of the NCXs coupled to H_1 receptors and HCN channels linked to H_2 receptors. As the reversal potential of NCXs is highly positive (Wu *et al.*, 2004; Zhang *et al.*, 2011), they are scarcely affected by small fluctuations of membrane potential, but their activation can provide an efficient force to depolarize neurons. Thus, through activation of NCXs coupled to H_1 receptors, histamine effectively depolarizes and increases spontaneous firing rates of the MVN
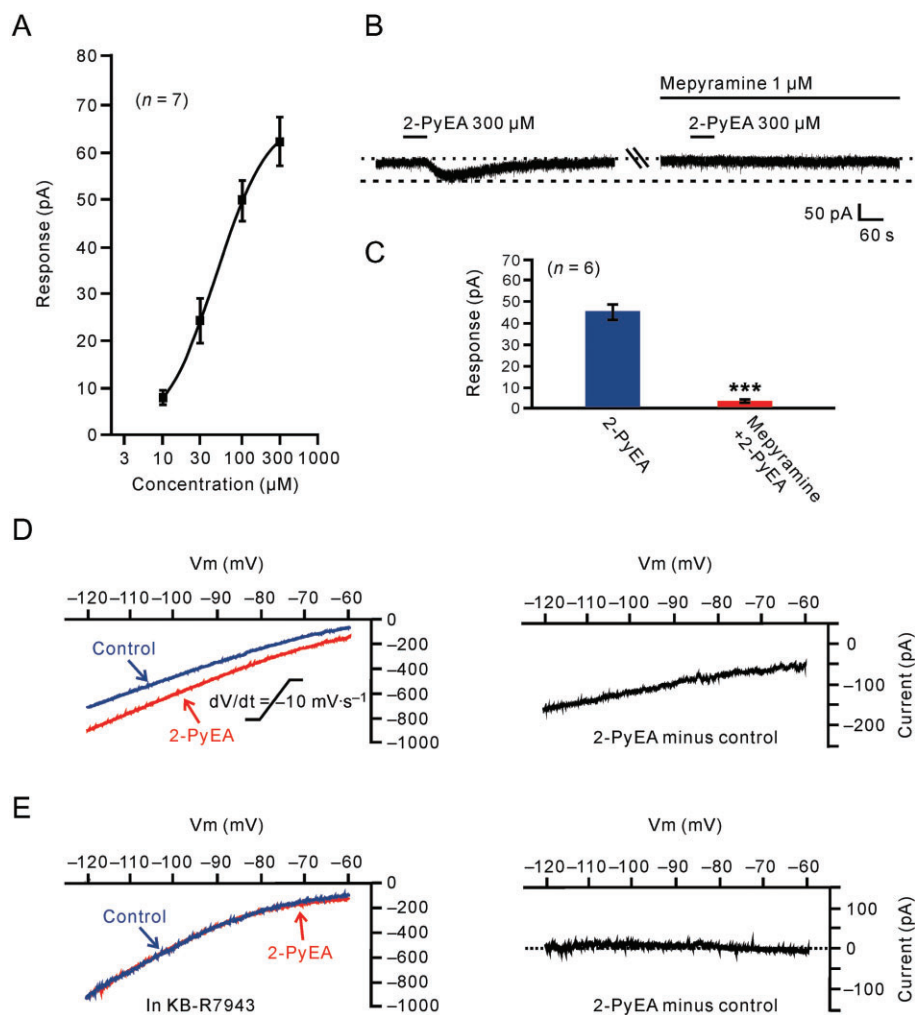
Figure 4
Histamine H_1 receptor-mediated inward current and its electrophysiological feature. (A) Concentration–response curve for 2-PyEA on seven recorded MVN neurons shows a mean EC_{50} value of 46.7 µM for 2-PyEA. (B) The 2-PyEA-induced inward current was totally blocked by mepyramine, indicating 2-PyEA evoked an isolated current associated with the activation of postsynaptic H_1 receptors. (C) Group data of the six tested MVN neurons. Data shown are means ± SEM; ***$P < 0.001$. (D, E) Slow ramp command tests ($dV/dt = -10$ mV·s^{-1}, ranged from −60 to −120 mV) were employed to evaluate the $I–V$ curves for a large voltage range in the absence and presence of 2-PyEA. The 2-PyEA-induced inward current had a larger amplitude at −120 mV as compared with −60 mV, and the two curves showed a trend of intersection at a potential more depolarized than −60 mV (the left panel in D). Subtracting the control from the current recorded during 2-PyEA application yielded a difference current representing the 2-PyEA-induced current (the right panel in D). In the presence of 50 µM KB-R7943, a selective blocker of NCXs, the $I–V$ curve recorded during 2-PyEA application coincided with that recorded in the absence of 2-PyEA (the left panel in E) and the 2-PyEA-induced current disappeared (the right panel in E).

neurons. On the other hand, HCN channels are usually referred to as 'pacemaker channels' (Pape, 1996) because they are activated during hyperpolarization and thus help accelerate depolarization to trigger a faster spike and generate neuronal rhythmic activity. Therefore, by opening of HCN channels coupled to H_2 receptors, histamine can quickly increase the excitability of MVN neurons and modulate their firing patterns, subsequently influencing vestibular reflexes through the MVN circuitry.

In addition to its key position in allergic responses in the periphery, now histamine is also widely considered to be a general modulator for whole brain activity. The central histaminergic system solely originates from the tuberomammil-

lary nucleus of the hypothalamus but extensively innervates almost the whole brain including the vestibular nuclei in the brainstem (Brown et al., 2001; Haas and Panula, 2003; Haas et al., 2008). Unilateral disruption of histaminergic neurotransmission with cimetidine (an H_2 receptor antagonist) or α-methylhistamine (an H_3 receptor agonist) in the vestibular nuclei leads to a postural and oculomotor syndrome similar to that seen after hemilabyrinthectomy (de Waele et al., 1992). Betahistine or thioperamide, another potent and selective H_3 receptor antagonist, reduce acute symptoms after vestibular deafferentation in rats (Pan et al., 1998) and improve recovery in cats (Tighilet et al., 2006; 2007). Similarly, chlorpheniramine, an H_1 receptor antagonist, was also reported to
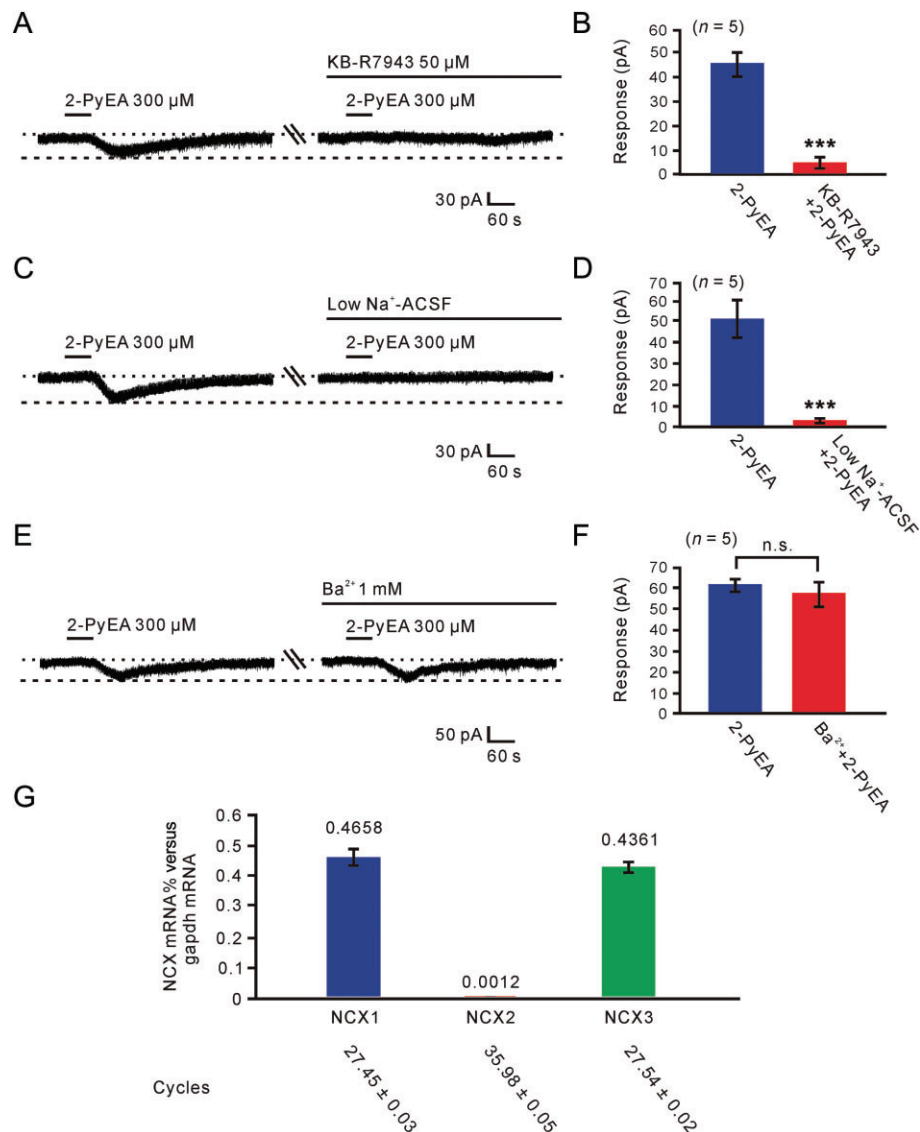
Figure 5
NCXs contributed to the histamine H_1-receptor-mediated inward current on MVN neurons. (A) The 2-PyEA-induced inward current was totally blocked by KB-R7943 in gap-free mode. (B) Group data of the five tested MVN neurons. (C, D) The 2-PyEA-induced inward current was totally blocked in low Na^+ ($Tris^+$) ACSF ($n = 5$). (E, F) Ba^{2+}, a broad spectrum blocker of K^+ channels, had no influence on the 2-PyEA-induced inward current ($n = 5$). Data shown are means ± SEM; n.s. indicates non-significant and ***$P < 0.001$, significant differences. (G) Bar graphs showing relative expression of NCX1, NCX2 and NCX3 mRNAs in the MVN.

accelerate vestibular compensation in hemilabyrinthectomized goldfish (Piratello and Mattioli, 2004). All these observations demonstrate a key position of hypothalamic histaminergic afferent inputs in vestibular functions and compensation.

The central histaminergic modulation of vestibular reflexes and functions is only one important component of the effects of the histaminergic system on motor control. Besides the vestibular nuclei in the brainstem, various critical subcortical motor structures, including the cerebellum (Shen *et al.*, 2002; Song *et al.*, 2006; He *et al.*, 2012) closely related to vestibular nuclei, also receive direct hypothalamic

histaminergic projections. Interestingly, without exception, neurons in all these subcortical motor centres are uniformly excited by histamine. As most histaminergic endings (varicosities) do not typically form synaptic specializations and almost all of the histamine receptors are metabotropic (Haas and Panula, 2003; Haas *et al.*, 2008), we suggest that histamine or histaminergic inputs from the hypothalamus to these central motor structures may not transmit fast signals, but act as a biasing force to influence electrophysiological properties of these motor neurons and hold their excitability and responsiveness at an appropriate level. In this way, the central histaminergic system may extensively modulates the
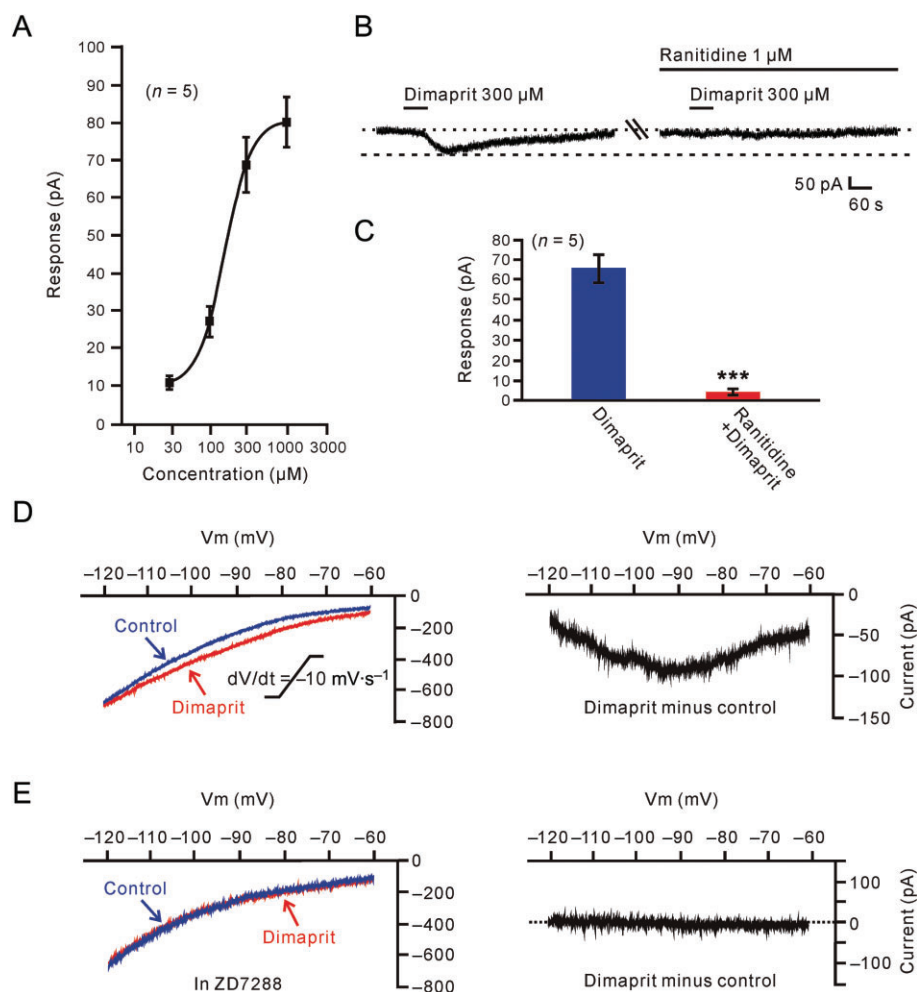
Figure 6

Histamine H_2 receptor-mediated inward current and its electrophysiological feature. (A) Concentration–response curve for dimaprit on five recorded MVN neurons shows the mean EC_{50} of 157.7 μM. (B) The dimaprit-induced inward current was abolished by ranitidine, indicating dimaprit evoked an isolated current associated with the activation of postsynaptic H_2 receptors. (C) Group data of the five tested MVN neurons. Data shown are means ± SEM; ***$P < 0.001$. (D, E) Slow ramp command tests were employed to obtain the I–V curves in the absence and presence of dimaprit (the left panel in D). The difference current representing the dimaprit-induced current (the right panel in D) exhibited a significant feature of hyperpolarization-activated non-selective cation current (via HCN channels). Under a condition of blockage of HCN channels by continuously applying ZD7288, the I–V curves recorded in the absence and presence of dimaprit coincided (the left panel in E) and the dimaprit-induced net current became zero (the right panel in E).

sensorimotor integration in circuits through various sub-cortical motor structures including the MVN and actively regulate movements. Actually, depletion of brain histamine or knockout of histamine receptors altered ambulatory activity and reduced exploratory behaviour (Onodera *et al.*, 1994; Inoue *et al.*, 1996; Toyota *et al.*, 2002). In the cerebellum, histamine and histaminergic afferents enhance muscle strength, influence footprints and improve motor balance and motor coordination (Song *et al.*, 2006; He *et al.*, 2012). Considering that the hypothalamus is still an important centre for autonomic and visceral regulation, we suggest that the hypothalamic histaminergic innervation of motor structures including the MVN may contribute significantly to somatic and non-somatic integration (Zhu *et al.*, 2006).

In summary, histamine regulates MVN function through presynaptic and postsynaptic actions, both of which hold key positions in the understanding of the physiological and pathophysiological significance of histaminergic modulation on vestibular functions. Moreover, other motor diseases, such as Parkinson's disease (Shan *et al.*, 2012) and Huntington's disease (van Wamelen *et al.*, 2011), are also related to local changes of both presynaptic and postsynaptic histamine receptors. Therefore, the roles of the NCXs and HCN channels coupled to postsynaptic H_1 and H_2 receptors on the MVN neurons in vestibular functions and dysfunctions need to be assessed further. The ion exchangers and channels linked to histamine receptors may become potential targets for the treatment of vestibular disorders as well as other motor diseases.
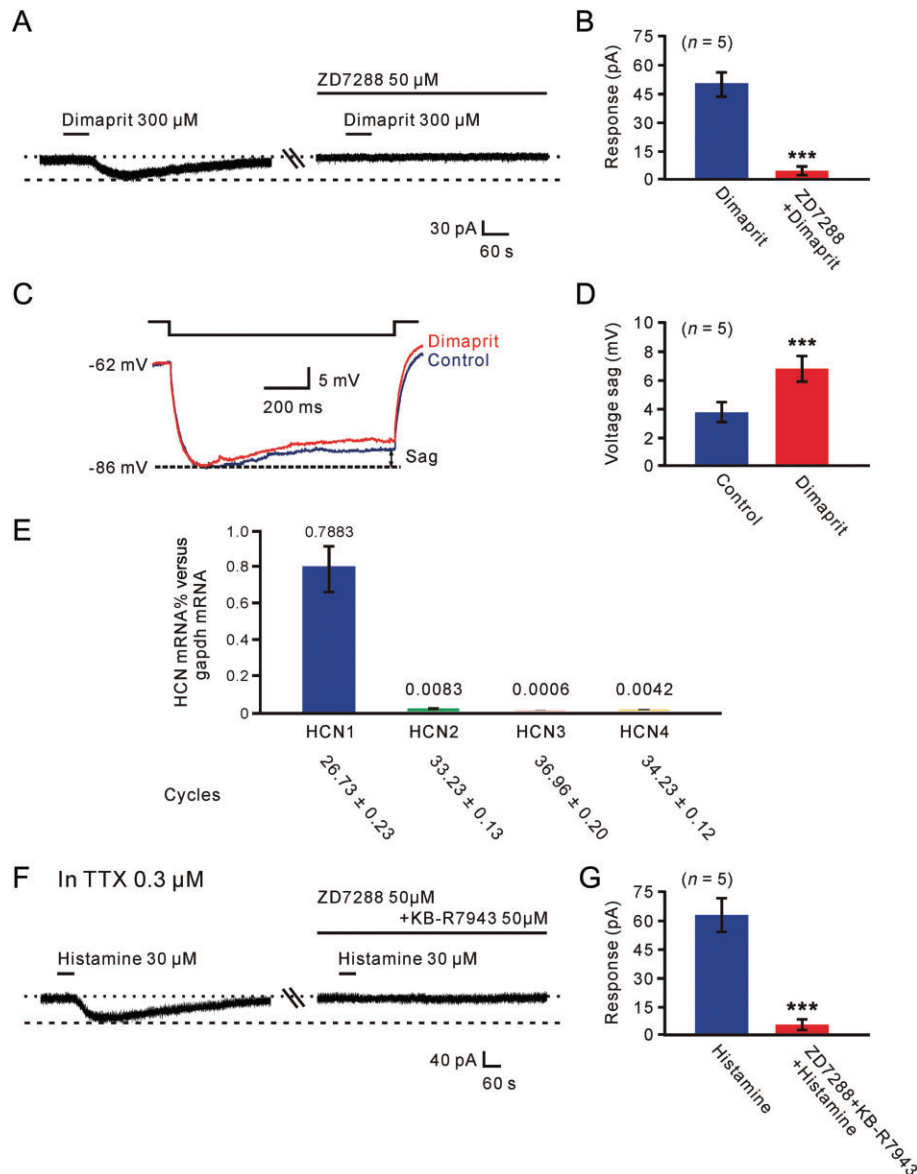
Figure 7

HCN channels mediated the histamine H_2-receptor-induced inward current on MVN neurons. (A) ZD7288 totally blocked the inward current induced by dimaprit. (B) Group data of the five tested MVN neurons. Data shown are means ± SEM; ***$P < 0.001$. (C) Neuron displayed inward rectification (sag) in response to a hyperpolarizing current pulse. Dimaprit (300 μM) increased the amplitude of the voltage sag. (D) Group data of the depolarizing sag of the five tested MVN neurons in the absence and presence of dimaprit. Data shown are means ± SEM; ***$P < 0.001$. (E) Bar graphs showing relative expression of HCN1, HCN2, HCN3 and HCN4 channel mRNAs in the MVN. (F) In the presence of TTX, combined application of ZD7288 and KB-R7943 totally blocked the histamine-induced postsynaptic inward current, indicating HCN channels and NCXs co-mediate the postsynaptic excitatory effect of histamine on MVN neurons. (G) Group data of the five tested MVN neurons. Data shown are means ± SEM; ***$P < 0.001$.

Acknowledgements

Conflicts of interest

None.

References

Alexander SP, Mathie A, Peters JA (2011). Guide to Receptors and Channels (GRAC), 5th edition. Br J Pharmacol 164 (Suppl. 1): S1–S324

Annunziato L, Pignataro G, Di Renzo GF (2004). Pharmacology of brain Na^+/Ca^{2+} exchanger: from molecular biology to therapeutic perspectives. Pharmacol Rev 56: 633–654.

Atherton JF, Kitano K, Baufreton J, Fan K, Wokosin D, Tkatch T et al. (2010). Selective participation of somatodendritic HCN channels in inhibitory but not excitatory synaptic integration in neurons of the subthalamic nucleus. J Neurosci 30: 16025–16040.

Beraneck M, Hachemaoui M, Idoux E, Ris L, Uno A, Godaux E et al. (2003). Long-term plasticity of ipsilesional medial vestibular nucleus neurons after unilateral labyrinthectomy. J Neurophysiol 90: 184–203.

Bergquist F, Dutia MB (2006). Central histaminergic modulation of vestibular function – a review. Sheng Li Xue Bao 58: 293–304.

Bergquist F, Ruthven A, Ludwig M, Dutia MB (2006). Histaminergic and glycinergic modulation of GABA release in the vestibular nuclei of normal and labyrinthectomised rats. J Physiol 577: 857–868.

Bolívar JJ, Tapia D, Arenas G, Castañón-Arreola M, Torres H, Galarraga E (2008). A hyperpolarization-activated, cyclic nucleotide-gated, (Ih-like) cationic current and HCN gene expression in renal inner medullary collecting duct cells. Am J Physiol Cell Physiol 294: C893–C906.

Bouthenet ML, Ruat M, Sales N, Garbarg M, Schwartz JC (1988). A detailed mapping of histamine H1-receptors in guinea-pig central nervous system established by autoradiography with [125I]iodobolpyramine. Neuroscience 26: 553–600.

Brown RE, Stevens DR, Haas HL (2001). The physiology of brain histamine. Prog Neurobiol 63: 637–672.

Connelly WM, Shenton FC, Lethbridge N, Leurs R, Waldvogel HJ, Faull RLM et al. (2009). The histamine H4 receptor is functionally expressed on neurons in the mammalian CNS. Br J Pharmacol 157: 55–63.

Gittis AH, du Lac S (2007). Firing properties of GABAergic versus non-GABAergic vestibular nucleus neurons conferred by a differential balance of potassium currents. J Neurophysiol 97: 3986–3996.

Gittis AH, du Lac S (2008). Similar properties of transient, persistent, and resurgent Na currents in GABAergic and non-GABAergic vestibular nucleus neurons. J Neurophysiol 99: 2060–2065.

Gittis AH, Moghadam SH, du Lac S (2010). Mechanisms of sustained high firing rates in two classes of vestibular nucleus neurons: differential contributions of resurgent Na, Kv3, and BK currents. J Neurophysiol 104: 1625–1634.

Haas H, Panula P (2003). The role of histamine and the tuberomamillary nucleus in the nervous system. Nat Rev Neurosci 4: 121–130.

Haas HL, Sergeeva OA, Selbach O (2008). Histamine in the nervous system. Physiol Rev 88: 1183–1241.

Hain TC, Uddin M (2003). Pharmacological treatment of vertigo. CNS Drugs 17: 85–100.

He YC, Wu GY, Li D, Tang B, Li B, Ding Y et al. (2012). Histamine promotes rat motor performances by activation of H_2 receptors in the cerebellar fastigial nucleus. Behav Brain Res 228: 44–52.

Highstein SM, Holstein GR (2006). The anatomy of the vestibular nuclei. Prog Brain Res 151: 157–203.

Inoue I, Yanai K, Kitamura D, Taniuchi I, Kobayashi T, Niimura K et al. (1996). Impaired locomotor activity and exploratory behavior in mice lacking histamine H1 receptors. Proc Natl Acad Sci USA 93: 13316–13320.

Jablonowski JA, Grice CA, Chai W, Dvorak CA, Venable JD, Kwok AK et al. (2003). The first potent and selective non-imidazole human histamine H4 receptor antagonists. J Med Chem 46: 3957–3960.

Johnston AR, MacLeod NK, Dutia MB (1994). Ionic conductances contributing to spike repolarization and after-potentials in rat medial vestibular nucleus neurones. J Physiol 481: 61–77.

Lacour M (2006). Restoration of vestibular function: basic aspects and practical advances for rehabilitation. Curr Med Res Opin 22: 1651–1659.

Lacour M, Sterkers O (2001). Histamine and betahistine in the treatment of vertigo: elucidation of mechanisms of action. CNS Drugs 15: 853–870.

Lazarov N, Rozloznik M, Reindl S, Rey-Ares V, Dutschmann M, Gratzl M (2006). Expression of histamine receptors and effect of histamine in the rat carotid body chemoafferent pathway. Eur J Neurosci 24: 3431–3444.

Lethbridge NL, Chazot PL (2010). Immunological identification of the mouse H4 histamine receptor on spinal cord motor neurons using a novel anti-mouse H4R antibody. Inflamm Res 59 (Suppl. 2): S197–S198.

Lim HD, Smits RA, Bakker RA, van Dam CM, de Esch IJ, Leurs R (2006). Discovery of S-(2-guanidylethyl)-isothiourea (VUF 8430) as a potent nonimidazole histamine H4 receptor agonist. J Med Chem 49: 6650–6651.

Lozada AF, Aarnisalo AA, Karlstedt K, Stark H, Panula P (2004). Plasticity of histamine H_3 receptor expression and binding in the vestibular nuclei after labyrinthectomy in rat. BMC Neurosci 5: 32.

Lu J, Tong XY, Wang XL (2002). Altered gene expression of Na^+/Ca^{2+} exchanger isoforms NCX1, NCX2 and NCX3 in chronic ischemic rat brain. Neurosci Lett 332: 21–24.

McGrath JC, Drummond GB, McLachlan EM, Kilkenny C, Wainwright CL (2010). Guidelines for reporting experiments involving animals: the ARRIVE guidelines. Br J Pharmacol 160: 1573–1576.

Notomi T, Shigemoto R (2004). Immunohistochemical localization of Ih channel subunits, HCN1-4, in the rat brain. J Comp Neurol 471: 241–276.

Onodera K, Yamatodani A, Watanabe T, Wada H (1994). Neuropharmacology of the histaminergic neuron system in the brain and its relationship with behavioral disorders. Prog Neurobiol 42: 685–702.

Palacios JM, Wamsley JK, Kuhar MJ (1981). The distribution of histamine H1-receptors in the rat brain: an autoradiographic study. Neuroscience 6: 15–37.

Pan JB, O'Neill AB, Hancock AA, Sullivan JP, Brioni JD (1998). Histaminergic ligands attenuate barrel rotation in rats following unilateral labyrinthectomy. Methods Find Exp Clin Pharmacol 20: 771–777.

Pape HC (1996). Queer current and pacemaker: the hyperpolarization-activated cation current in neurons. Annu Rev Physiol 58: 299–327.

Paxinos G, Watson C (2007). The Rat Brain in Stereotaxic Coordinates, 6th edn. Academic Press: San Diego, CA.

Peng SY, Zhuang QX, He YC, Zhu JN, Wang JJ (2013). Histamine excites neurons of the inferior vestibular nucleus in rats by activation of H_1 and H_2 receptors. Neurosci Lett 541: 87–92.

Pillot C, Heron A, Cochois V, Tardivel-Lacombe J, Ligneau X, Schwartz JC et al. (2002). A detailed mapping of the histamine H_3 receptor and its gene transcripts in rat brain. Neuroscience 114: 173–193.

Piratello AC, Mattioli R (2004). Effects of chlorpheniramine and L-histidine on vestibular compensation in goldfish, Carassius auratus. Neurosci Lett 367: 160–163.

Ruat M, Traiffort E, Arrang JM, Leurs R, Schwartz JC (1991). Cloning and tissue expression of a rat histamine H2-receptor gene. Biochem Biophys Res Commun 179: 1470–1478.

Serafin M, Khateb A, de Waele C, Vidal PP, Mühlethaler M (1990). Low threshold calcium spikes in medial vestibular nuclei neurones in vitro: a role in the generation of the vestibular nystagmus quick phase in vivo? Exp Brain Res 82: 187–190.

Serafin M, de Waele C, Khateb A, Vidal PP, Mühlethaler M (1991). Medial vestibular nucleus in the guinea-pig. II. Ionic basis of the intrinsic membrane properties in brainstem slices. Exp Brain Res 84: 426–433.

Serafin M, Khateb A, Vibert N, Vidal PP, Mühlethaler M (1993). Medial vestibular nucleus in the guinea-pig: histaminergic receptors. I. An in vitro study. Exp Brain Res 93: 242–248.

Shan L, Bossers K, Luchetti S, Balesar R, Lethbridge N, Chazot PL et al. (2012). Alterations in the histaminergic system in the substantia nigra and striatum of Parkinson's patients: a postmortem study. Neurobiol Aging 33: 1488. e1–e13.

Shen B, Li HZ, Wang JJ (2002). Excitatory effects of histamine on cerebellar interpositus nuclear cells of rats through H_2 receptors in vitro. Brain Res 948: 64–71.

Song YN, Li HZ, Zhu JN, Guo CL, Wang JJ (2006). Histamine improves rat rota-rod and balance beam performances through H_2 receptors in the cerebellar interpositus nucleus. Neuroscience 140: 33–43.

Straka H, Vibert N, Vidal PP, Moore LE, Dutia MB (2005). Intrinsic membrane properties of vertebrate vestibular neurons: function, development and plasticity. Prog Neurobiol 76: 349–392.

Strakhova MI, Nikkel AL, Manelli AM, Hsieh GC, Esbenshade TA, Brioni JD et al. (2009). Localization of histamine H4 receptors in the central nervous system of human and rat. Brain Res 1250: 41–48.

Tighilet B, Trottier S, Mourre C, Lacour M (2006). Changes in the histaminergic system during vestibular compensation in the cat. J Physiol 573: 723–739.

Tighilet B, Mourre C, Trottier S, Lacour M (2007). Histaminergic ligands improve vestibular compensation in the cat: behavioural, neurochemical and molecular evidence. Eur J Pharmacol 568: 149–163.

Tiligada E, Kyriakidis K, Chazot PL, Passani MB (2011). Histamine pharmacology and new CNS drug targets. CNS Neurosci Ther 17: 620–628.

Toyota H, Dugovic C, Koehl M, Laposky AD, Weber C, Ngo K et al. (2002). Behavioral characterization of mice lacking histamine H_3 receptors. Mol Pharmacol 62: 389–397.

Vizuete ML, Traiffort E, Bouthenet ML, Ruat M, Souil E, Tardivel-Lacombe J et al. (1997). Detailed mapping of the histamine H2 receptor and its gene transcripts in guinea-pig brain. Neuroscience 80: 321–343.

de Waele C, Serafin M, Khateb A, Vibert N, Yabe T, Arrang JM et al. (1992). An in vivo and in vitro study of the vestibular nuclei histaminergic receptors in the guinea pig. Ann N Y Acad Sci 656: 550–565.

van Wamelen DJ, Shan L, Aziz NA, Anink JJ, Bao AM, Roos RA et al. (2011). Functional increase of brain histaminergic signaling in Huntington's disease. Brain Pathol 21: 419–427.

Wang JJ, Dutia MB (1995). Effects of histamine and betahistine on rat medial vestibular nucleus neurones: possible mechanism of action of anti-histaminergic drugs in vertigo and motion sickness. Exp Brain Res 1995: 18–24.

Wu M, Zaborszky L, Hajszan T, van den Pol AN, Alreja M (2004). Hypocretin/orexin innervation and excitation of identified septohippocampal cholinergic neurons. J Neurosci 24: 3527–3536.

Yabe T, de Waele C, Serafin M, Vibert N, Arrang JM, Mühlethaler M et al. (1993). Medial vestibular nucleus in the guinea-pig: histaminergic receptors. II. An in vivo study. Exp Brain Res 93: 249–258.

Zhang J, Han XH, Li HZ, Zhu JN, Wang JJ (2008). Histamine excites rat lateral vestibular nuclear neurons through activation of post-synaptic H2 receptors. Neurosci Lett 448: 15–19.

Zhang J, Li B, Yu L, He YC, Li HZ, Zhu JN et al. (2011). A role for orexin in central vestibular motor control. Neuron 69: 793–804.

Zhu JN, Yung WH, Kwok-Chong Chow B, Chan YS, Wang JJ (2006). The cerebellar-hypothalamic circuits: potential pathways underlying cerebellar involvement in somatic-visceral integration. Brain Res Rev 52: 93–106.

Zhuang QX, Wu YH, Wu GY, Zhu JN, Wang JJ (2013). Histamine excites rat superior vestibular nuclear neurons via postsynaptic H_1 and H_2 receptors in vitro. Neurosignals 21: 174–183.